

Article

Speed of Sound Measurements of Biogas from a Landfill Biomethanation Process

José Juan Segovia ¹, Alejandro Moreau ¹, Xavier Paredes ¹, Teresa E. Fernández-Vicente ², David Vega-Maza ¹ and María Carmen Martín ^{1,*}

¹ TERMOCAL Research Group, Research Institute on Bioeconomy, Escuela de Ingenierías Industriales, Universidad de Valladolid, Paseo del Cauce 59, 47011 Valladolid, Spain

² Centro Español de Metrología, Alfar 2, 28760 Tres Cantos, Madrid, Spain

* Correspondence: mcarmen.martin@uva.es; Tel.: +34-983-423-756

Abstract: Biogas is drawing attention as it can be a solution both to increase the renewable energy for heat or power supply and to help achieve a decarbonized economy. In this work, the measurements of the speed of sound of three mixtures of biogas from the biomethanation plant of the municipal waste of Valdemingómez, Madrid (Spain), are presented. The measurements were performed using an acoustic resonator, which is able to measure the speed of sound of gas mixtures with a relative expanded uncertainty of approximately 0.08%. A virial-type equation was also applied to fit the experimental values of the speed of sound, and the heat capacities as perfect gas were derived with uncertainties below 0.8%. In addition, the experimental results were compared with those calculated with the reference equations of state for natural gas mixtures such as GERG-2008 and AGA8-DC92. For both equations, the average relative deviations were less than 0.02% and 0.2% for the speed of sound and the heat capacities, respectively. These values are less than the uncertainties of these equations, demonstrating their reliability in predicting the thermodynamic behavior of biogas.

Keywords: biogas; speed of sound; acoustic resonator

Citation: Segovia, J.J.; Moreau, A.; Paredes, X.; Fernández-Vicente, T.E.; Vega-Maza, D.; Martín, M.C. Speed of Sound Measurements of Biogas from a Landfill Biomethanation Process. *Energies* **2023**, *16*, 2068. <https://doi.org/10.3390/en16042068>

Academic Editor: Attilio Converti

Received: 12 January 2023

Revised: 9 February 2023

Accepted: 18 February 2023

Published: 20 February 2023



Copyright: © 2023 by the authors. Licensee MDPI, Basel, Switzerland. This article is an open access article distributed under the terms and conditions of the Creative Commons Attribution (CC BY) license (<https://creativecommons.org/licenses/by/4.0/>).

1. Introduction

Anaerobic digestion of organic material by microorganisms results in the production of biogas under anaerobic conditions. In recent years, this treatment, as applied to waste and residues from agriculture and industry, municipal organic waste, sewage sludge, etc., has become as one of the most attractive renewable energy pathways. Biogas is a renewable fuel that can be utilized to produce heat and electricity or as a vehicle fuel [1]. However, the composition of raw biogas is mainly CH₄ (50% to 60%) and CO₂ (40% to 50%), as well as other gases, such as N₂, CO, O₂, H₂, H₂O, or H₂S, which involves an upgrading treatment to obtain biomethane of higher purity; this process implies CO₂ removal, desulfurization, or dehumidification [2]. The purification level depends on the final application of the biogas; more impurities are admissible for electrical energy production in gas turbines than, for example, for injection into the natural gas grid, which requires a purity of methane greater than 95% [3]. The use of biogas as an alternative energy gas is being promoted by European energy policy to increase the presence of renewable energy and as a measure to decarbonize the economy.

This study is focused on the biomethanation plant “La Paloma” of the Valdemingómez landfill, Madrid (Spain). Raw biogas (2000 Nm³/h) is upgraded using a water scrubber technique to remove H₂S and CO₂. This facility is the first in Spain that injects the biogas into the national gas network. This plant produces 5 × 10⁶ Nm³/year of biomethane. There is also a cogeneration plant that uses the biogas as fuel.

This work is part of our research interest in the thermodynamic characterization of new energy gases. Accurate knowledge of the thermodynamic properties of these mixtures is of great importance for the design and optimization of all the involved processes, such as production, transport, and storage. Moreover, the speed of sound is an important thermophysical property that is widely used to characterize these mixtures, as it provides information about the medium through which it passes [4,5]. The speed of sound can be measured or calculated with equations of state, so accurate experimental data are essential to test the reliability of the equations of state. Additionally, the speed of sound of these gas mixtures is needed to calibrate the flow meters, which use sonic nozzles [6]. Rahmouni et al. [7] presented a methodology using speed of sound, among other properties, to control the composition of the biogas during combustion.

Scarce data are available on the speed of sound in natural-gas-like mixtures. Natural gas mixtures were measured by Ewing and Goodwin [8], Labes et al. [9], and Younglove et al. [10]. Other authors have measured synthetic mixtures; for example, Costa-Gomes and Trusler [11] measured a five-component mixture, Ahmadi et al. [12] performed measurements for a seven-component mixture, and our group previously published measurements of speed of sound for a synthetic mixture of four components [13].

The novelty of this work is that the presented speed of sound measurements correspond to three real biogas samples. The samples were taken in different stages of the biomethanation process and were characterized to verify both the performance of the process and the thermodynamic models used for natural-gas-like mixtures, such as the AGA8-DC92 [14] and the GERG-2008 [15,16] equations of state.

2. Materials and Methods

2.1. Materials

As mentioned, the samples under study were taken at three different stages of the process: the first sample is a raw mixture collected from the outlet of the digesters where the biogas is produced by anaerobic digestion of organic waste (“Raw biogas”), the second mixture comes from the intermediate step of the backwashing process to reduce the concentration of carbon dioxide (“Washed biogas”), and the third biogas mixture is the final product (“Biomethane”) when the upgrading process is completed by pressure swing adsorption (PSA) just before its injection into the natural gas grid. The samples were delivered in 5 L stainless-steel bottles with pressures not higher than 0.2 MPa.

The composition of the samples and the corresponding uncertainties are summarized in Table 1. The mixtures were analyzed by gas chromatography in an external laboratory.

Table 1. Molar composition (x_i) and expanded ($k = 2$) uncertainty ($U(x_i)$) of the three samples from the biomethanation plant of the Valdemingómez landfill in Madrid (Spain).

Compound	Raw Biogas		Washed Biogas		Biomethane	
	x_i	$U(x_i)$	x_i	$U(x_i)$	x_i	$U(x_i)$
Methane	0.60145	0.00047	0.72874	0.00032	0.96494	0.00020
Carbon Dioxide	0.39198	0.00071	0.26403	0.00085	0.01856	0.00017
Carbon Monoxide	0.000010	0.000006	0.000010	0.000006	0.000010	0.000006
Oxygen	0.000010	0.000006	0.00404	0.00023	0.00300	0.00011
Nitrogen	0.002011	0.000058	0.002021	0.000058	0.01348	0.00026
Hydrogen	0.000010	0.000006	0.000010	0.000006	0.000010	0.000006
Pentane	0.00021	0.00012	0.00021	0.00012	-	-
Isopentane	0.00021	0.00012	0.00021	0.00012	-	-
Hexane	0.00019	0.00011	0.00019	0.00011	-	-
Hydrogen Sulfide	0.001227	0.000042	0.000530	0.000008	-	-

2.2. Equipment

Measurements of speed of sound in these mixtures were carried out using a spherical resonator manufactured at Imperial College on London based on the design of Trusler and Ewing [17]. A detailed description can be found in references [13,18], but the main features of the technique are described below. Figure 1 shows a picture of the resonator and its schematic view.

Two aligned hemispheres made of grade 321 austenitic stainless steel and welded by electron beam form the spherical resonant cavity, the nominal radius of which is 40 mm, with a thickness of 11 mm. The two transducers used as source and detector are placed on the inner surface of the north shell. The source transducer is fed by the wave generator, whereas the exit signal of the transducer detector is preamplified and supplied to a lock-in; the relative standard uncertainty of frequency measurement is below 1 part in 10^6 .

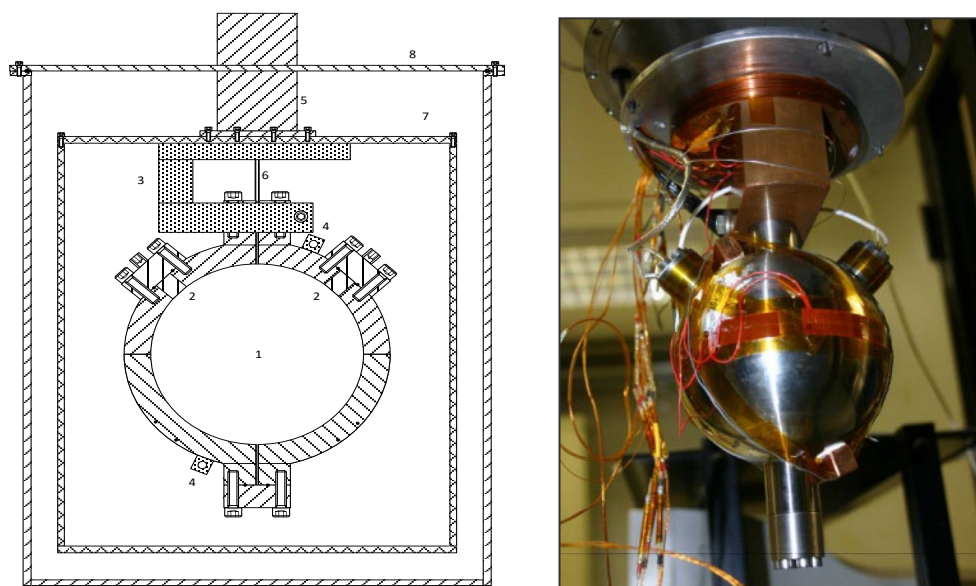


Figure 1. A schematic view of the spherical resonator [18]: 1, spherical cavity; 2, acoustic transducers; 3, copper block where the sphere is suspended; 4, thermoresistance holders; 5, main structure; 6, inlet/outlet pipe; 7, thermostatic vessel; 8, vacuum vessel. On the right is a picture of the resonator.

The resonator is maintained at a constant temperature using a system with different stages and three temperature control loops. A first control is performed on the copper block from which the cavity is hung; the heat flow provided from the copper block to the resonator is controlled with a heater and a platinum resistance thermometer, maintaining the set temperature for the experiment. Two capsule-type platinum resistance thermometers located on the north and south hemispheres are used to measure the mean temperature of the gas through an ac bridge, with an estimated standard uncertainty of 2 mK. The heat transfer between the resonant cavity and the shield is minimized by the vacuum induced between the two in a radiation trap. To operate below ambient temperature, the system is immersed in a Dewar vessel, which is fed with ethanol from an external thermostatic bath.

The pressure is measured by means of a piezoelectric quartz transducer, which is placed on the top of the gas inlet tube. The relative standard uncertainty of the pressure sensor is 0.01%.

The cylinder is charged with the gas mixture from the bottle. Once the pressure is suitable, the spherical resonator temperature is set to the measuring conditions. The measurements were carried out isothermally at different temperatures: the spherical resonator is initially full of gas at the highest pressure; then, the pressure is reduced for each measuring point.

2.3. Speed of Sound Calculation

The experimental technique does not measure speed of sound directly, but the acoustic resonance frequency is related to the speed of sound (w). In the case of a spherical cavity, the relation is expressed as Equation (1) [4]:

$$w = (2\pi a f_{lm}) / \vartheta_{lm} \quad (1)$$

where a is the inner radius of the cavity, and f_{lm} is the frequency of resonance for the “ lm ” mode, ϑ_{lm} is the eigenvalue for the “ lm ” acoustic resonance mode. The measured magnitude is the frequency; the eigenvalues are calculated according to Bessel’s spherical equations [10]. The internal radius of the spherical resonator must be calculated and is determined by measuring the resonance frequencies for argon [18], the equation of state and speed of sound of which are well known [19].

Equation (1) is completely true for a perfect spherical cavity. However, some corrections of frequency should be taken into account, such as the thermal boundary layer, bulk viscosity, shell coupling, and holes in the shell, due to imperfections of the cavity. The correctness of the above acoustic model is assessed by evaluation of the dispersion of the speed of sound and the difference between the experimental and the calculated resonance half-widths and the excess half-widths (Δg), defined as:

$$\Delta g = g_{exp} - g_{calc} = g_{exp} - (g_{th} + g_{cl} + g_0) \quad (2)$$

where g_{th} is the heat losses in the thermal boundary layer, g_{cl} is the classical viscous and thermal energy losses in the bulk of the fluid, and g_0 is the energy dissipation in the inlet and blind gas ducts.

3. Results

The speed of sound is related to thermodynamic properties according to the following definition (3):

$$w^2 = \left(\frac{\partial p}{\partial \rho} \right)_S \quad (3)$$

where p is pressure, ρ is the mass density, and S is entropy.

For a perfect gas, the speed of sound is

$$w^2 = RT\gamma^{pg}/M \quad (4)$$

in which R is the gas constant, T is temperature, $\gamma^{pg} = c_p^{pg}/c_v^{pg}$ stands for the perfect gas–heat capacity ratio, and M is the molar mass of the mixture.

When sound is continuously produced in a closed cavity, the acoustic wave forms a standing wave; if the frequency of this wave generated by a source coincides with one of the natural frequencies (normal modes of vibration) of the cavity, resonance is produced. The simplified acoustic model for a spherical cavity allows for calculation of the speed of sound using the resonance frequencies of the gas-filled spherical resonator through the radial natural modes. In our measurement procedure, the first four acoustic radial modes, i.e., (0, 2), (0, 3), (0, 4), and (0, 5), are recorded; the speeds of sound reported in Table 2 were obtained from the average of these four values.

The measurements were performed at temperatures between 273 K and 325 K corresponding to the working temperature range of the technique; this is also the same range as that used in our laboratory for a synthetic biogas mixture [13], enabling a comparison between the two datasets.

For these mixtures, the main contributions to the overall uncertainty come from the uncertainty of the gas composition and the determination of the sphere radius through speed of sound measurements in argon.

Moreover, the experimental results were compared with the AGA8-DC92 [14] and GERG-2008 [15,16] equations of state; these values were obtained using NIST REFPROP 10.0 software (Reference fluid thermodynamic and transport properties database) [20].

Table 2. Experimental speeds of sound (w_{exp}) of the three studied biogas mixtures, relative expanded ($k = 2$) uncertainty ($U_r(w_{\text{exp}})$), and relative differences ($\Delta w_{r,\text{EoS}} = (w_{\text{exp}} - w_{\text{EoS}})/w_{\text{EoS}}$) from the speeds of sound predicted by the AGA8-DC92 and GERG-2008 Equations of State.

p/MPa	$w_{\text{exp}}/\text{m}\cdot\text{s}^{-1}$	$10^6 \cdot U_r(w_{\text{exp}})$	$10^6 \cdot \Delta w_{r,\text{AGA}}$	$10^6 \cdot \Delta w_{r,\text{GERG}}$
Raw Biogas at $T = 300.00 \text{ K}$				
0.74302	342.108	735	234	161
0.69614	342.318	728	217	149
0.59837	342.756	734	190	132
0.50091	343.182	729	197	149
0.39619	343.684	724	81	46
0.29868	344.107	724	108	84
0.19898	344.533	724	154	144
0.15288	344.737	730	159	155
Washed Biogas at $T = 273.00 \text{ K}$				
0.78036	350.855	924	115	69
0.71455	351.216	917	113	64
0.61725	351.753	919	107	55
0.52538	352.260	946	101	46
0.42046	352.840	915	99	42
0.31978	353.397	912	98	40
0.21686	353.963	910	111	52
0.14440	354.444	912	−111	−169
Washed Biogas at $T = 325.00 \text{ K}$				
0.77172	382.184	939	−19	−129
0.71425	382.346	938	−41	−149
0.61857	382.603	937	−36	−141
0.52221	382.890	943	−102	−204
0.41324	383.197	937	−122	−219
0.31511	383.490	935	−178	−269
0.21595	383.765	931	−172	−258
0.14771	383.957	947	−172	−254
Biomethane at $T = 325.00 \text{ K}$				
0.84447	454.778	479	−59	28
0.77356	454.943	477	−135	−52
0.70564	455.077	471	−153	−75
0.62046	455.260	471	−205	−133
0.51741	455.434	472	−154	−88
0.41480	455.629	471	−145	−86
0.32008	455.750	517	0.4	53

Standard uncertainties ($k = 1$): $u_r(p) = 0.0001$; $u(T) = 2 \text{ mK}$.

For a real gas, the squared speed of sound data can be fitted to a virial-type equation of state (5):

$$w^2(p, T) = A_0 + A_1 p + A_2 p^2 + \dots \quad (5)$$

where $A_0 = \gamma^{\text{pg}} RT/M$, $A_1 = \gamma^{\text{pg}} \beta_a(T)/M$, $A_2 = \gamma^{\text{pg}} (\gamma_a(T) - B(T) \beta_a(T))/MRT$, β_a stands for the second acoustic virial coefficient, γ_a stands for the third acoustic virial coefficient, and B stands for the density second virial coefficient.

The results of this fitting are reported in Table 3, which also includes a comparison with the data predicted by the AGA8-DC92 [14] and GERG-2008 [15,16] equations of state using REFPROP software [20].

Table 3. Perfect gas–heat capacity ratio (γ^{pg}), perfect gas–heat capacities at constant volume (c_v^{pg}) and at constant pressure (c_p^{pg}), and second virial acoustic coefficients (β_a) of the three biogas mixtures with their corresponding relative expanded ($k = 2$) uncertainties and relative deviations of these properties ($\Delta X_{r,\text{EoS}} = (X_{\text{exp}} - X_{\text{EoS}})/X_{\text{EoS}}$) from the predicted values with AGA8-DC92 and GERG-2008 equations of state.

	X_{exp}	$U_r(X_{\text{exp}})/\%$	$\Delta X_{r,\text{AGA}}/\%$	$\Delta X_{r,\text{GERG}}/\%$
Raw Biogas at $T = 300.00$ K				
γ^{pg}	1.2958	0.13	−0.04	−0.03
$c_v^{\text{pg}}/\text{J}\cdot\text{mol}^{-1}\cdot\text{K}^{-1}$	28.11	0.58	0.17	0.14
$c_p^{\text{pg}}/\text{J}\cdot\text{mol}^{-1}\cdot\text{K}^{-1}$	36.42	0.59	0.13	0.11
$\beta_a/\text{m}^3\cdot\text{mol}^{-1}$	-641.7×10^{-7}	0.78	−0.64	−1.8
Washed Biogas at $T = 273.00$ K				
γ^{pg}	1.2958	0.13	−0.04	−0.03
$c_v^{\text{pg}}/\text{J}\cdot\text{mol}^{-1}\cdot\text{K}^{-1}$	28.11	0.58	0.17	0.14
$c_p^{\text{pg}}/\text{J}\cdot\text{mol}^{-1}\cdot\text{K}^{-1}$	36.42	0.59	0.13	0.11
$\beta_a/\text{m}^3\cdot\text{mol}^{-1}$	-641.7×10^{-7}	0.78	−0.64	−1.8
Washed Biogas at $T = 325.00$ K				
γ^{pg}	1.2883	0.18	0.04	0.05
$c_v^{\text{pg}}/\text{J}\cdot\text{mol}^{-1}\cdot\text{K}^{-1}$	28.84	0.79	−0.19	−0.21
$c_p^{\text{pg}}/\text{J}\cdot\text{mol}^{-1}\cdot\text{K}^{-1}$	37.16	0.81	−0.15	−0.17
$\beta_a/\text{m}^3\cdot\text{mol}^{-1}$	-399.9×10^{-7}	1.4	−0.45	−1.4
Biomethane at $T = 325.00$ K				
γ^{pg}	1.29282	0.076	−0.01	−0.01
$c_v^{\text{pg}}/\text{J}\cdot\text{mol}^{-1}\cdot\text{K}^{-1}$	28.395	0.33	0.10	0.03
$c_p^{\text{pg}}/\text{J}\cdot\text{mol}^{-1}\cdot\text{K}^{-1}$	36.709	0.34	0.09	0.03
$\beta_a/\text{m}^3\cdot\text{mol}^{-1}$	-224.7×10^{-7}	3.9	−9.0	−7.7

4. Discussion

In order to complete the comparison between the experimental results and the data calculated with the equations of state, Table 4 summarizes some statistical parameters, and the deviations presented in Table 2 are depicted in Figure 2.

Table 4. Statistical parameters for the comparison between the experimental values of the speed of sound and those calculated with the AGA8-DC92 and GERG-2008 equations of state.

	Deviation from AGA/Parts in 10^6				Deviation from GERG/Parts in 10^6			
	AAD	Bias	RMS	MaxD	AAD	Bias	RMS	MaxD
Raw Biogas at $T = 300$ K	167	167	175	234	128	128	133	161
Washed Biogas at $T = 273$ K	107	79	107	115	67	25	78	169
Washed Biogas at $T = 325$ K	105	−105	122	178	203	−203	210	269
Biomethane at $T = 325$ K	122	−122	137	205	74	−51	80	133

According to the results of the comparison, the deviations are less than the uncertainties of both the experimental data and the equations of state themselves. Nevertheless, the trend of negative deviations at higher temperatures was also observed for this kind of mixtures in a previous work [13]. In this limited range of study, both equations behave similarly, as can be deduced from the results presented in Table 4.

On the other hand, the deviations of the experimental values from both equations of state, as can be seen in Figure 2, shown a similar trend. However, the AGA8-DC92 equation gives a maximum positive deviation of 243 parts in 10^6 for the “raw biogas” mixture at the highest pressure versus a maximum positive deviation of 161 parts in 10^6 from GERG-2008 predictions for the same mixture under the same pressure. In terms of negative deviations, the extreme values of deviations are -269 parts in 10^6 from GERG-2008 for the “washed biogas” at $p \sim 0.3$ MPa and $T = 325$ K and -205 parts in 10^6 from AGA8-DC92 for the “biomethane” sample at $p \sim 0.6$ MPa and $T = 325$ K.

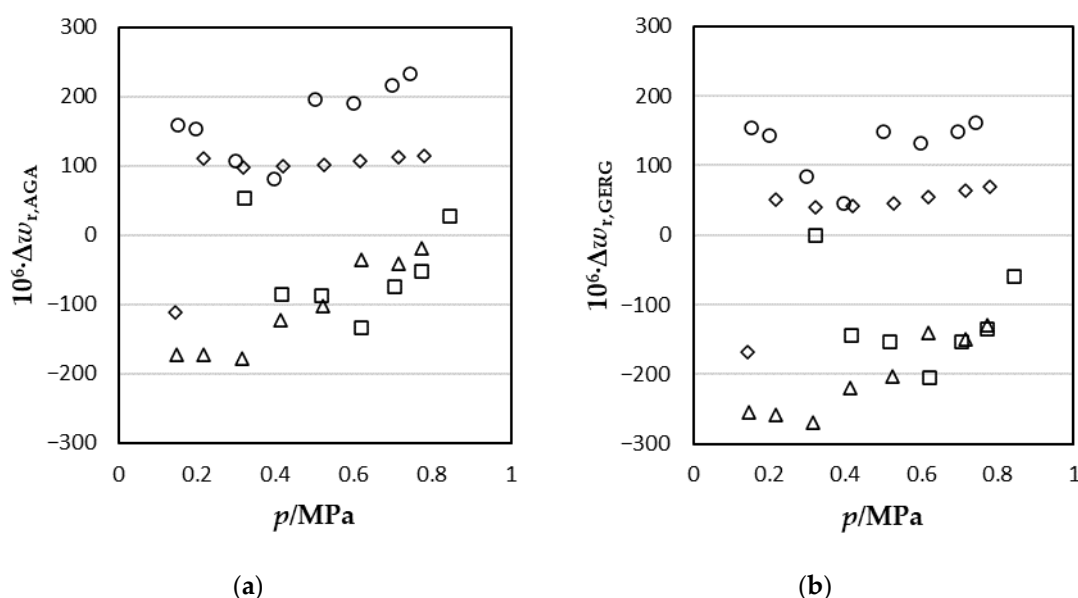


Figure 2. Relative deviations of the speed of sound ($\Delta w_{r,EoS} = (w_{exp} - w_{EoS})/w_{EoS}$) from the values predicted by equations of state as a function of pressure: (a) AGA8-DC92 and (b) GERG-2008. Each mixture and isotherm are represented with a different symbol: (○) raw biogas at $T = 300$ K; (◇) washed biogas at $T = 273$ K; (Δ) washed biogas at $T = 325$ K; (□) biomethane at $T = 325$ K.

As mentioned in the Introduction, there are few papers in the literature dealing with this type of mixture. Ewing and Goodwin [8] measured the speed of sound of a natural gas mixture using a spherical resonator. The methane mole fraction was close to 0.94, and these data were obtained at $T = 255$ K in the pressure range of 0.064 to 6.1 MPa, with a standard uncertainty in the speed of sound of 70 parts in 10^6 . Their results were compared to six equations of state (AGA8-85, AGA8-92, GERG-88, NGAS NIST, DDMIX, and Supertrapp), and the lowest relative deviations were obtained from NGAS EoS, with differences between -320 and $+260$ parts in 10^6 and within the uncertainty of the equation. These deviations agree with our findings.

The speeds of sound of two natural gas mixtures with nominal molar compositions ($\{CH_4 (0.884) + C_2H_6 (0.052) + N_2 (0.032) + \text{traces}\}$ and $\{CH_4 (0.896) + C_2H_6 (0.084) + N_2 (0.012) + \text{traces}\}$) at pressures between 12 and 70 MPa in the temperature range of 263 to 413 K were determined out by Labes et al. [9] with a pulse-echo technique, the estimated uncertainty of which was 600 parts in 10^6 . These results were used to test cubic EoS, chain rotator EoS, SBR EoS, Lee–Kesler correlation, and AGA8 EoS. The best absolute average deviations were obtained for AGA8 EoS ($<0.7\%$). In this case, the pressure range is much larger than in the previous study, so greater experimental uncertainty and larger deviations from predictions are to be expected.

Younglove et al. [10] measured the speeds of sound of four natural gases from Gulf Coast, Amarillo, Statoil Dry Gas, and Statoil Statvordgass suppliers. A cylindrical resonator with a standard uncertainty of 250 parts in 10^6 was used for the measurements, which were extended to the temperature range of 250 to 350 K and pressures up to 10 MPa. Data

were compared to NGAS NIST and AGA8 EoS, agreeing both models within the range of model uncertainty, except at the lowest isotherm, i.e., $T = 250$ K and above 5 MPa.

A synthetic five-component mixture ($\{\text{CH}_4 (0.80) + \text{N}_2 (0.10) + \text{C}_2\text{H}_6 (0.05) + \text{C}_3\text{H}_8 (0.03) + \text{CO}_2 (0.02)\}$) was thermodynamically characterized by Costa-Gomes and Trusler [11] through speed of sound measurements using a spherical resonator. The data were obtained at temperatures from 250 to 350 K and pressures between 0.1 and 20 MPa with an uncertainty in speed of sound of 300 parts in 10^6 . The relative deviations of the AGA8 equation of state were generally within 0.2%.

Ahmadi et al. [12] measured the density and speed of sound of a synthetic gas comprising seven components: $\{\text{CH}_4 (0.879) + \text{C}_2\text{H}_6 (0.060) + \text{C}_3\text{H}_8 (0.020) + \text{CO}_2 (0.020) + \text{N}_2 (0.015) + \text{C}_4\text{H}_{10} (0.003) + \text{i-C}_4\text{H}_{10} (0.002)\}$. The speed of sound was obtained using a cylindrical acoustic cell working in ultrasonic spectra. They determined five isotherms between 323 K and 415 K at pressures up to 58 MPa. They observed an average deviation of 0.11% from the values predicted by GERG-2008, with a maximum value of 0.6%. The average deviation was within the uncertainty of the equation, but the temperature and pressure ranges do not match ours.

In a previous work [13], a synthetic mixture of biogas ($\{\text{CH}_4 (0.498) + \text{CO}_2 (0.351) + \text{N}_2 (0.100) + \text{CO} (0.005)\}$) was studied by measuring the speed of sound using the same technique. These measurements were undertaken at $p = 1\text{--}12$ MPa and $T = 273, 300$, and 325 K with an average expanded ($k = 2$) relative uncertainty of 165 parts in 10^6 . The relative deviations of GERG-2008 predictions had a mean value of 0.06%, which is below the uncertainty of the model; however, a particular trend was observed for the different isotherms. At $T = 273$ K, GERG-2008 predicts higher values of speed of sound than the experimental ones, and the discrepancies increase at high pressure, reaching a maximum of 0.3% at $p = 11.5$ MPa; on the contrary, at $T = 325$ K, the model predicts lower values of speed of sound up to -0.07% at the lowest pressure. When these results are compared with those obtained for the real biogas samples studied in this work, smaller deviations from the GERG-2008 equation are observed.

Finally, our experimental data were also fitted to a virial-type equation (5). The root mean square of the residuals is 31 parts in 10^6 for the raw biogas at $T = 300$ K, 84 parts in 10^6 for the washed biogas at $T = 273$ K, 17 parts in 10^6 for the washed biogas at $T = 325$ K, and 56 parts in 10^6 for the biomethane mixture at $T = 325$ K, which are much lower than the experimental uncertainty.

The parameters of the adjustment allow for estimation of the perfect gas–heat capacity ratio, the perfect gas–heat capacities at constant volume and at constant pressure, and the second virial acoustic coefficient (see Table 3). The average absolute relative deviation for c_p^{pg} and c_p^{pg} is 0.12%, whereas the experimental expanded ($k = 2$) uncertainty estimated by the Monte Carlo method [21] ranges from 0.33 to 0.81%, i.e., about three to eight times larger than the AAD value. AGA8-DC92 and GERG-2008 equations of state show a better agreement with the measurements.

On the other hand, the relative deviations of the second virial acoustic coefficient from the values obtained with the two equations of state are not consistent within the experimental uncertainty, and both models overestimate this coefficient. The disagreement might be due to the pressure range of the measurements. The highest working pressure of 0.9 MPa was imposed by the small amount of gas in the 5 L sample bottles supplied at 0.2 MPa after extraction from the biogas plant.

5. Conclusions

Novel speed of sound measurements were performed for three different biogas mixtures: raw biogas obtained from digestors (methane: 60%); washed biogas collected after the scrubbing unit (methane: 73%); and “biomethane” (methane 96%), which is the final product ready to be injected in the gas grid. The samples are representative of key stages of the biomethanation plant of Valdemingómez landfill, Madrid (Spain).

The data were obtained using a spherical resonator, which is one of the most accurate techniques available to determine this important thermophysical property at temperatures between 273 and 325 K and pressures up to 0.9 MPa. There is a lack of experimental data on biogas mixtures in the literature; however, such data are crucial to determine the behavior of such new energy gases and how the reference equations of state predict it.

That is why the experimental results were compared to AGA8-DC92 and GERG-2008 equations of state, obtaining relative absolute average deviations (AAD) of 125 and 118 parts in 10^6 for the AGA8-DC92 and GERG-2008 EoS, respectively. These values are less than both the uncertainties of the measurements and the models. The good agreement between our experimental results and those predicted with both models allow us to deduce the goodness of these equations in predicting the behavior of biogas for very different compositions such as the three studies samples.

Finally, the experimental data were fitted to the acoustic virial equation truncated after first order with an average root mean square value of the residuals lower than 47 parts in 10^6 , which is much lower than the experimental uncertainty. The heat capacities as perfect gas for the three mixtures were also calculated from the fitting, and our results were in good agreement with the values predicted by AGA8-DC92 and GERG-2008.

Author Contributions: Conceptualization, J.J.S. and M.C.M.; formal analysis, J.J.S., A.M., X.P. and D.V.-M.; supervision, J.J.S.; resources, T.E.F.-V.; writing—review and editing, M.C.M.; project administration J.J.S. and M.C.M. All authors have read and agreed to the published version of the manuscript.

Funding: This research was funded by the Regional Government OF Castilla Y León and EU-FEDER, VA280P18, and CLU-2019-04.

Data Availability Statement: Data are available upon request.

Acknowledgments: D.V.M. acknowledges his “Beatriz Galindo Senior” fellowship (BEA-GAL18/00259). X.P. acknowledges his “María Zambrano” fellowship.

Conflicts of Interest: The authors declare no conflict of interest.

References

1. Scarlat, N.; Dallemand, J.F.; Fahl, F. Author 1, A.B.; Author 2, C.D. Biogas: Developments and perspectives in Europe. *Renew. Energy* **2018**, *129*, 457–472. <https://doi.org/10.1016/j.rene.2018.03.006>.
2. Muñoz, R.; Meier, L.; Diaz, I.; Jeison, D. A review on the state-of-the-art of physical/chemical and biological technologies for biogas upgrading. *Rev. Environ. Sci. Biotechnol.* **2015**, *14*, 727–759. <https://doi.org/10.1007/s11157-015-9379-1>.
3. Awe, O.W.; Zhao, Y.; Nzihou, A.; Minh, D.P.; Lyczko, N. A Review of Biogas Utilisation, Purification and Upgrading Technologies. *Waste Biomass Valor.* **2017**, *8*, 267–283. <https://doi.org/10.1007/s12649-016-9826-4>.
4. Trusler, J.P.M. *Physical Acoustics and Metrology of Fluids*; Adam Hilger: Bristol, UK, 1991.
5. Prikhod'koa, I.V.; Samarova, A.A.; Toikka, A.M. On Application of PC-SAFT Model for Estimating the Speed of Sound in Synthetic and Natural Oil-and-Gas Mixtures. *Russian J. Appl. Chem.* **2019**, *92*, 262–266.
6. Farzaneh-Gord, M.; Mohseni-Gharyehsafa, B.; Arabkoohsar, A.; Ahmadi, M.H.; Sheremet, M.A. Precise prediction of biogas thermodynamic properties by using ANN algorithm. *Ren. Energy* **2020**, *147*, 179–191. <https://doi.org/10.1016/j.renene.2019.08.112>.
7. Rahmouni, C.; Tazerout, M.; Le Corre, O. A method to determine biogas composition for combustion control. In Proceedings of the SAE Technical Papers 2002 International Spring Fuels and Lubricants Meeting and Exhibition, Reno, NV, USA, 6–9 May 2002. <https://doi.org/10.4271/2002-01-1708>.
8. Ewing, M.B.; Goodwin, A.R.H. Speeds of sound in a natural gas of specified composition at the temperature 255 K and pressures in the range 64 kPa to 6.1 MPa. *J. Chem. Thermodyn.* **1993**, *25*, 1503–1511. <https://doi.org/10.1006/jcht.1993.1150>.
9. Labes, P.; Daridon, J.L.; Lagourette, B.; Saint-Guirons, H. Measurement and prediction of ultrasonic speed under high pressure in natural gases. *Int. J. Thermophys.* **1994**, *15*, 803–819. <https://doi.org/10.1007/BF01447096>.
10. Younglove, B.A.; Frederick, N.V.; McCarty, R.D. *Speed of Sound Data and Related Models for Mixtures of Natural Gas Constituents*; National Institute of Standards and Technology (NIST): Boulder, U.S.A., 1993. <https://doi.org/10.6028/NIST.MONO.178>.
11. Costa-Gomes, M.F.; Trusler, J.P.M. The speed of sound in two methane-rich gas mixtures at temperatures between 250 K and 350 K and at pressures up to 20 MPa. *J. Chem. Thermodyn.* **1998**, *30*, 1121–1129. <https://doi.org/10.1006/jcht.1998.0378>.
12. Ahmadi, P.; Chapoy, A.; Tohidi, B. Density, speed of sound and derived thermodynamic properties of a synthetic natural gas. *J. Nat. Gas Sci. Tech.* **2017**, *40*, 249–266. <https://doi.org/10.1016/j.jngse.2017.02.009>.

13. Lozano-Martín, D.; Segovia, J.J.; Martín, M.C.; Fernández-Vicente, T.; del Campo, D. Speeds of sound for a biogas mixture $\text{CH}_4 + \text{N}_2 + \text{CO}_2 + \text{CO}$ from $p = (1\text{--}12)$ MPa at $T = (273, 300 \text{ and } 325)$ K measured with a spherical resonator. *J. Chem. Thermodyn.* **2016**, *102*, 348–356. <https://doi.org/10.1016/j.jct.2016.07.033>.
14. AGA Report No. 8 Part 1 *Thermodynamic Properties of Natural Gas and Related Gases*; American Gas Association: Washington, DC, USA, 2017.
15. Kunz, O.; Klimeck, R.; Wagner, W.; Jaeschke, M. *The GERG-2004 Wide-Range Equation of State for Natural Gases and Other Mixtures*; GERG TM15; Fortschr.-Ber. VDI, Reihe 6, Nr. 557; VDI Verlag: Düsseldorf, Germany, 2007.
16. Kunz, O.; Wagner, W. The GERG-2008 wide-range equation of state for natural gases and other mixtures: An expansion of GERG-2004. *J. Chem. Eng. Data* **2012**, *57*, 3032–3091. <https://doi.org/10.1021/je300655b>.
17. Ewing, M.B.; Trusler, J.P.M. Speed of sound in CF_4 between 175 and 300 K measured with a spherical resonator. *J. Chem. Phys.* **1989**, *90*, 1106–1115. <https://doi.org/10.1063/1.456165>.
18. Pérez-Sanz, F.J.; Segovia, J.J.; Martín, M.C.; del Campo, D.; Villamañán, M.A. Speeds of sound in $(0.95 \text{ N}_2 + 0.05 \text{ CO}$ and $0.9 \text{ N}_2 + 0.1 \text{ CO})$ gas mixtures at $T = (273 \text{ and } 325)$ K and pressure up to 10 MPa. *J. Chem. Thermodyn.* **2014**, *79*, 224–229. <https://doi.org/10.1016/j.jct.2014.07.022>.
19. Tegeler, C.S.R.; Wagner, W. A new equation of state for argon covering the fluid region for temperatures from the melting line to 700K at pressures up to 1000 MPa. *J. Phys. Chem. Ref. Data* **1999**, *28*, 779–850. <http://dx.doi.org/10.1063/1.556037>.
20. Lemmon, E.W.; Bell, I.H.; Huber, M.L.; McLinden, M.O. *NIST Standard Reference Database 23: Reference Fluid Thermodynamic and Transport Properties-REFPROP*; Version 10.0; National Institute of Standards and Technology Standard Reference Data programs; National Institute of Standards and Technology (NIST): Boulder, CO, USA, 2018.
21. Joint Committee for Guides in Metrology. *Evaluation of Measurement Data—Supplement 1 to the “Guide to the Expression of Uncertainty in Measurement”—Propagation of Distributions Using a Monte Carlo Method*; JCGM 101:2008; BIMP: Sèvres, France, 2008.

Disclaimer/Publisher’s Note: The statements, opinions and data contained in all publications are solely those of the individual author(s) and contributor(s) and not of MDPI and/or the editor(s). MDPI and/or the editor(s) disclaim responsibility for any injury to people or property resulting from any ideas, methods, instructions or products referred to in the content.